

Relativistic and Ultra-Relativistic Electron Bursts in Earth's Magnetotail Observed by Low-Altitude Satellites

Xiao-Jia Zhang^{1,2}, Anton V. Artemyev², Xinlin Li^{3,4}, Harry Arnold⁵, Vassilis Angelopoulos², Drew L. Turner⁵, Mykhaylo Shumko⁵, Andrei Runov², Yang Mei^{3,4}, Zheng Xiang⁴

¹Department of Physics, The University of Texas at Dallas, Richardson, TX, USA

²University of California, Los Angeles, Los Angeles, USA

³Laboratory for Atmospheric and Space Physics, University of Colorado Boulder, Boulder, CO, USA

⁴Department of Aerospace Engineering Sciences, University of Colorado Boulder, Boulder, CO, USA

⁵The Johns Hopkins University Applied Physics Laboratory, Laurel, MD USA

Key Points:

- We report observations of relativistic and ultra-relativistic electrons in near-Earth magnetotail
- We show energy spectra of relativistic electron bursts in the magnetotail
- We discuss potential mechanisms responsible for the formation of relativistic and ultra-relativistic electrons

arXiv:2408.17299v1 [physics.space-ph] 30 Aug 2024

Corresponding author: Xiao-Jia Zhang, xjzhang@utdallas.edu

Abstract

Earth’s magnetotail, a night-side region characterized by stretched magnetic field lines and strong plasma currents, is the primary site for the release of magnetic field energy and its transformation into plasma heating and kinetic energy plus charged particle acceleration during magnetic reconnection. In this study, we demonstrate that the efficiency of this acceleration can be sufficiently high to produce populations of relativistic and ultra-relativistic electrons, with energies up to several MeV, which exceeds all previous theoretical and simulation estimates. Using data from the low altitude ELFIN and CIRBE CubeSats, we show multiple events of relativistic electron bursts within the magnetotail, far poleward of the outer radiation belt. These bursts are characterized by power-law energy spectra and can be detected during even moderate substorms.

Plain Language Summary

Charged particle acceleration during magnetic field line reconnection is a universal process occurring in various space plasma environments. Traditionally, theoretical and simulation models of this acceleration are verified using data from the reconnection region in the near-Earth magnetosphere, where in-situ spacecraft measurements are most accessible. In this study, we demonstrate that the efficiency of this acceleration can significantly exceed previous estimates, leading to the formation of electron populations with energies up to several MeV, even in regions where thermal electron energies are below 1 keV. These observations of highly energetic electron bursts are made available by new low-altitude CubeSat missions monitoring magnetotail electron fluxes.

1 Introduction

The primary mechanism of charged particle acceleration in Earth’s magnetotail, the night-side region of the magnetosphere, is presumably related to near-Earth magnetotail reconnection (Baker et al., 1996; Angelopoulos, McFadden, et al., 2008; Paschmann et al., 2013). Numerous theoretical and observational investigations have focused on charged particle acceleration in near-Earth reconnection, because it determines the energy flux transported into the inner magnetosphere, which further supports the ring current and outer radiation belt (see discussions in Angelopoulos, Artemyev, et al., 2020; Lin et al., 2021; Jun et al., 2021; Hua et al., 2023; Kim et al., 2023).

Numerical simulations of electron acceleration in realistic magnetotail magnetic field configurations (see Birn et al., 2004; Ashour-Abdalla et al., 2011; Sorathia et al., 2018) usually combine the test particle approach (due to the negligible feedback of the high-energy (non-thermal), low-flux population on electromagnetic fields) with global MHD models that can reproduce the main elements of magnetotail dynamics. These simulations demonstrate the dominant role of adiabatic (Fermi and betatron) mechanisms in electron energization, which can accelerate electrons up to 100 – 200keV in the magnetotail (Zhou et al., 2011; Birn et al., 2013). Consistent with these model results, spacecraft observations confirm that effective electron acceleration due to magnetotail reconnection is largely contributed by electron acceleration at dipolarization fronts (Vaivads et al., 2011; Fu et al., 2013), which are the leading edges of fast plasma flows carrying enhanced magnetic fields and strong electric fields (Nakamura et al., 2002; Runov et al., 2009; Sitnov et al., 2009). These fronts can heat pre-accelerated electrons adiabatically via magnetic field line compression (Ashour-Abdalla et al., 2011, 2013; Pan et al., 2012), producing electrons with energies $\sim 100 - 300\text{keV}$ (Fu et al., 2019). Although further electron acceleration up to $\sim 1\text{ MeV}$ is possible during plasma injections into the inner magnetosphere (Sorathia et al., 2018; Turner, Cohen, Michael, et al., 2021), existing magnetotail models mostly focus on reproducing sub-relativistic (100–200 keV) electron fluxes. This upper limit at sub-relativistic energies in magnetotail simulations is likely dictated by available observations: majority of energetic electron measurements in the

outer magnetosphere are limited to sub-relativistic energies, $\sim 200 - 300\text{keV}$ (Imada et al., 2007; Øieroset et al., 2002; Retinò et al., 2008; Huang et al., 2012; Cohen et al., 2021; Ergun et al., 2020). But in reality, can electron acceleration in the magnetotail be more effective, and what are the actual upper energies of accelerated electrons? Historical observations in the distant tail by ISEE-3 (Slavin et al., 1992; Richardson et al., 1993) and in the middle tail by Imp 8 (Baker & Stone, 1977) reveal the presence of bursts of relativistic electrons, with energies of $\sim 0.2 - 2\text{MeV}$, although the geomagnetic context and origin of these bursts remain largely unknown.

This question is challenging to address with near-equatorial observations, because of the quite transient nature of electron acceleration in the magnetotail and the typical upper energy limit of energetic particle detectors onboard magnetotail missions (Wilken et al., 2001; Angelopoulos, Sibeck, et al., 2008; Blake et al., 2016), which lack high resolution in relativistic energies. A promising alternative is the new generation of low-altitude CubeSat missions with high energy resolutions. These CubeSats can quickly cross the field lines conjugate to the entire near-Earth’s magnetotail within a few minutes, effectively monitoring energetic electron populations in this region (Artemyev et al., 2022). Here we analyze several events where relativistic (above 500keV) and ultra-relativistic (several MeV) electron bursts were observed in Earth’s magnetotail by Colorado Inner Radiation Belt Experiment (CIRBE) (Li et al., 2024) and Electron Losses and Fields Investigation (ELFIN) (Angelopoulos, Tsai, et al., 2020) CubeSats. These observations likely represent the first clear separation of electron populations accelerated in the magnetotail and relativistic electron leakage from the outer radiation belt. We analyze the electron energy spectra and discuss possible mechanisms for such effective electron acceleration.

2 ELFIN observations

The two identical ELFIN CubeSats are equipped with an energetic particle detector (EPD) that measures electrons within the $[50, 6000]\text{keV}$ energy range across sixteen logarithmically distributed channels, with full pitch-angle coverage (22.5° angular bin) and 3s spin resolution (Angelopoulos, Tsai, et al., 2020). The pitch-angle resolution allows for the separation of locally trapped fluxes (j_{trap}) from precipitating (within the bounce loss cone) fluxes (j_{prec}), where j_{trap} is outside of the bounce loss cone and j_{prec} is within it. The ratio $j_{\text{prec}}/j_{\text{trap}}$ is useful in determining the specific magnetospheric region along the ELFIN track: the outer radiation belt is characterized by high j_{trap} of relativistic electrons and a low $j_{\text{prec}}/j_{\text{trap}}$ ratio, with transient bursts of $j_{\text{prec}}/j_{\text{trap}}$ due to wave driven electron precipitation; in contrast, the plasma sheet region exhibits significant j_{trap} only below $\sim 200 - 300\text{keV}$ and a $j_{\text{prec}}/j_{\text{trap}} \sim 1$ due to strong magnetic field line curvature scattering (see details in Mourenas et al., 2021; Angelopoulos et al., 2023). During its routine operation from December 2019 to September 2022, ELFIN detected several events with bursty increases of significant j_{trap} at energies up to a few MeVs within the plasma sheet. One such event is shown in Fig. 1(a,b): the black arrow marks the nominal plasma sheet region with electron fluxes at moderate energies ($< 300\text{keV}$). Within this region, there is a burst of relativistic fluxes with energies reaching up to $\sim 5\text{MeV}$. This burst is well separated from the outer radiation belt region and cannot be associated with the relativistic electron leakage (outward diffusion); instead, it is more likely generated by a local and highly effective acceleration mechanism. The inner edge of the plasma sheet, the electron isotropy boundary, as characterized by energy-latitude dispersion of $j_{\text{prec}}/j_{\text{trap}} \sim 1$ (see Sergeev et al., 2012; Wilkins et al., 2023), is located within $[60, 64^\circ]$, well equatorward from the relativistic electron burst. During this burst, the electron fluxes exceed the upper limit of ELFIN EPD, leading to a high background level (see X.-J. Zhang et al., 2022, for discussion of this effect during relativistic microbursts measured by ELFIN in the outer radiation belt). For spins with such a high background level, $j_{\text{prec}}/j_{\text{trap}}$ can show misleading variations, so we set it to 1.

The ELFIN relativistic burst event in Fig. 1(a,b) was observed when MMS (Burch et al., 2016) was in the night-side magnetosphere, detecting substorm electron injections as evidenced in energetic electron fluxes (note that MMS was 3 hours of MLT closer to midnight than ELFIN A): panels (d-f) show magnetic field perturbations (Russell et al., 2016), plasma flow speed (Young et al., 2016), and energetic electron fluxes (Blake et al., 2016) typical for substorm injections observed at latitudes away from the equator (see, e.g., discussion in Gabrielse et al., 2019). Therefore, ELFIN observations are associated with substorm activities (as confirmed by the AE index in panel (c)), including magnetic field-line reconnection, charged particle acceleration, and subsequent injection into the inner magnetosphere (see Birn et al., 2012; Gonzalez & Parker, 2016; Sitnov et al., 2019, and references therein). However, MMS' energetic electron detector does not capture an increase in relativistic electron fluxes (with the main flux increase being below 500keV), suggesting that the ELFIN-detected electron burst is likely spatially localized in MLT or may not reach lower L -shells (although MMS is projected far in the magnetotail due to a large B_x magnitude, the significant uncertainties of the magnetic field model in the night-side injection region suggest that it might be mapped closer to its instantaneous location at $\sim 6.7R_E$), possibly being scattered and lost into the atmosphere.

Figure 2 shows six examples of similar events from ELFIN, where bursts of relativistic electron fluxes up to 5MeV were detected well within the magnetotail, poleward from the outer radiation belt (black arrows in each event mark the latitudinal range of the magnetotail, poleward from the outer radiation belt). These events are associated with substorm activities (see AE profiles), but many of them occur during moderate AE levels ($< \sim 300$ nT). Therefore, we can infer that electron acceleration to relativistic energies in the magnetotail does not necessarily require specific geomagnetic conditions (e.g., intense substorm activity). However, due to limited ELFIN telemetry (a few orbits per day; see details in Tsai & et al., 2024), estimating the occurrence rate of such relativistic bursts is challenging in the ELFIN dataset. Moreover, all detected relativistic bursts are associated with very high background levels of the ELFIN EPD (see discussion in Angelopoulos et al., 2023; Tsai & et al., 2024). Thus, a detailed analysis of the electron spectra during such events cannot be conducted using the ELFIN dataset. However, it reveals an important characteristic of these bursts: their isotropic pitch-angle distributions, with $j_{prec}/j_{trap} \sim 1$. Therefore, measurements of locally trapped fluxes are sufficient to (1) estimate the precipitating relativistic electron fluxes from the magnetotail, and (2) compare with equatorial flux measurements from missions like MMS and THEMIS. Such isotropy is expected because electrons at these high energies are rapidly scattered by magnetic field line curvature in the magnetotail current sheet.

3 CIRBE observations

CIRBE is a 3U CubeSat equipped with the Relativistic Electron and Proton Telescope integrated little experiment-2 (REPTile-2) (Khoo et al., 2022; Li et al., 2022), measuring electrons within the [250, 6000]keV energy range across sixty channels with a time resolution of 1 sec (Li et al., 2024; Li, 2024). REPTile-2 has a field-of-view of 51° and a look direction nearly perpendicular to the background magnetic field, making it well-suited to measure perpendicular (90°) fluxes, i.e., the locally-trapped flux, j_{trap} (see discussion in Zhang et al., 2020). We analyzed CIRBE measurements during the prolonged storm interval, 4-7 November 2023, when CIRBE detected multiple relativistic electron bursts in near-Earth magnetotail. Although CIRBE does not resolve pitch-angle distributions, we may use the analogy of CIRBE and ELFIN measurements to distinguish the magnetotail region. To confirm that CIRBE's measurements of relativistic bursts are within the magnetotail, we also compare these measurements with precipitating and trapped electron fluxes measured by one of nearby POES satellites (Evans & Greer, 2004), which are traditionally used to localize the magnetotail/outer radiation belt transition region (e.g. Sergeev et al., 2012). Two main advantages of CIRBE measurements are (1) ex-

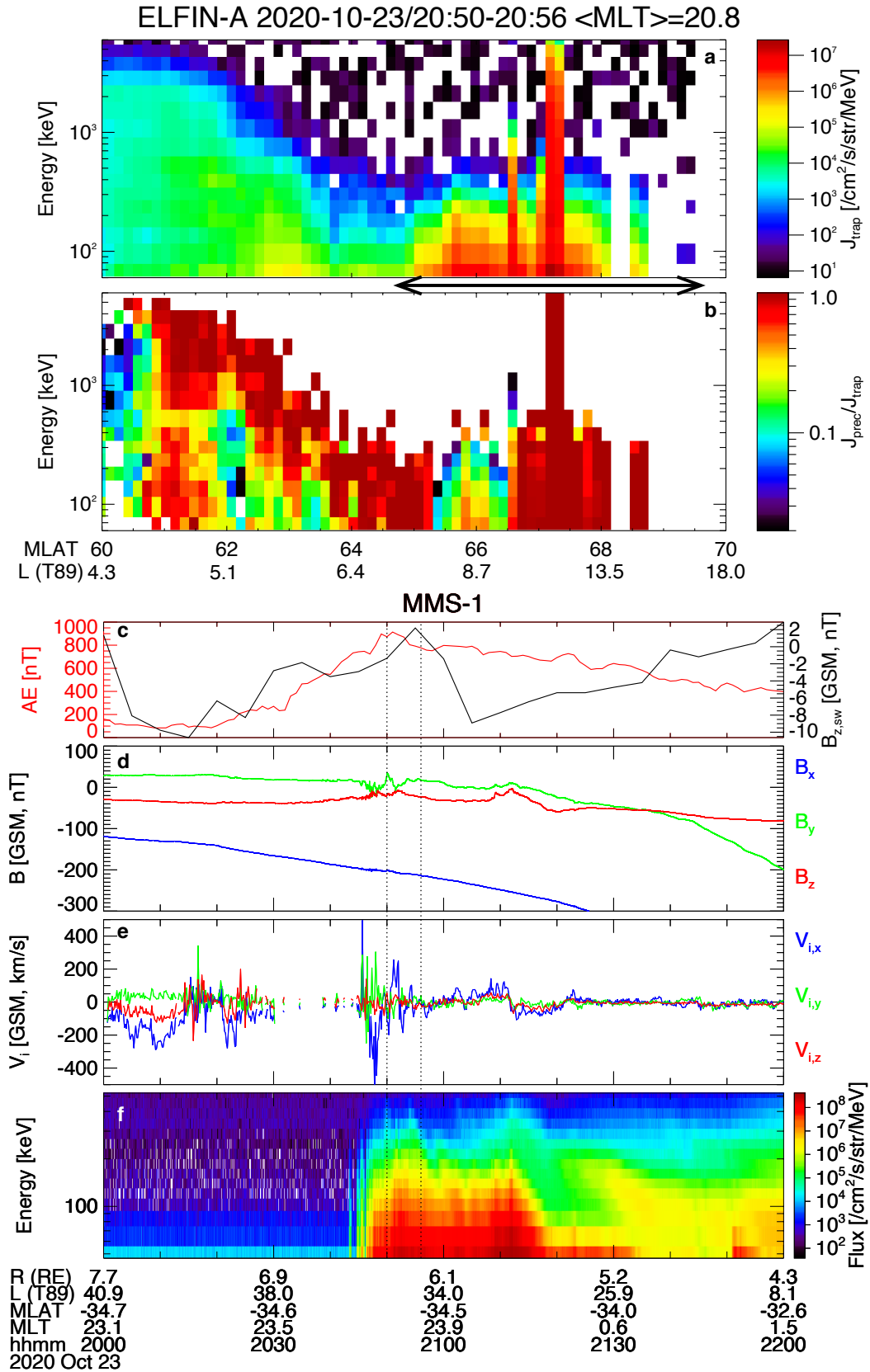


Figure 1. Overview of one ELFIN event with relativistic electron observations in near-Earth magnetotail on 23 October 2020, at $\sim 20:53$ UT. Panels (a, b) show locally trapped electron fluxes and precipitating-to-trapped flux ratio (versus magnetic latitude). The black arrow marks the plasma sheet region along the ELFIN track. Panel (c) shows AE index and solar wind B_z for the 2h interval embedding the ELFIN event. Panels (d,e,f) show MMS observations in the magnetotail: GSM magnetic field from (Russell et al., 2016), GSM plasma flows from (Young et al., 2016), and energetic electron spectra from (Blake et al., 2016).

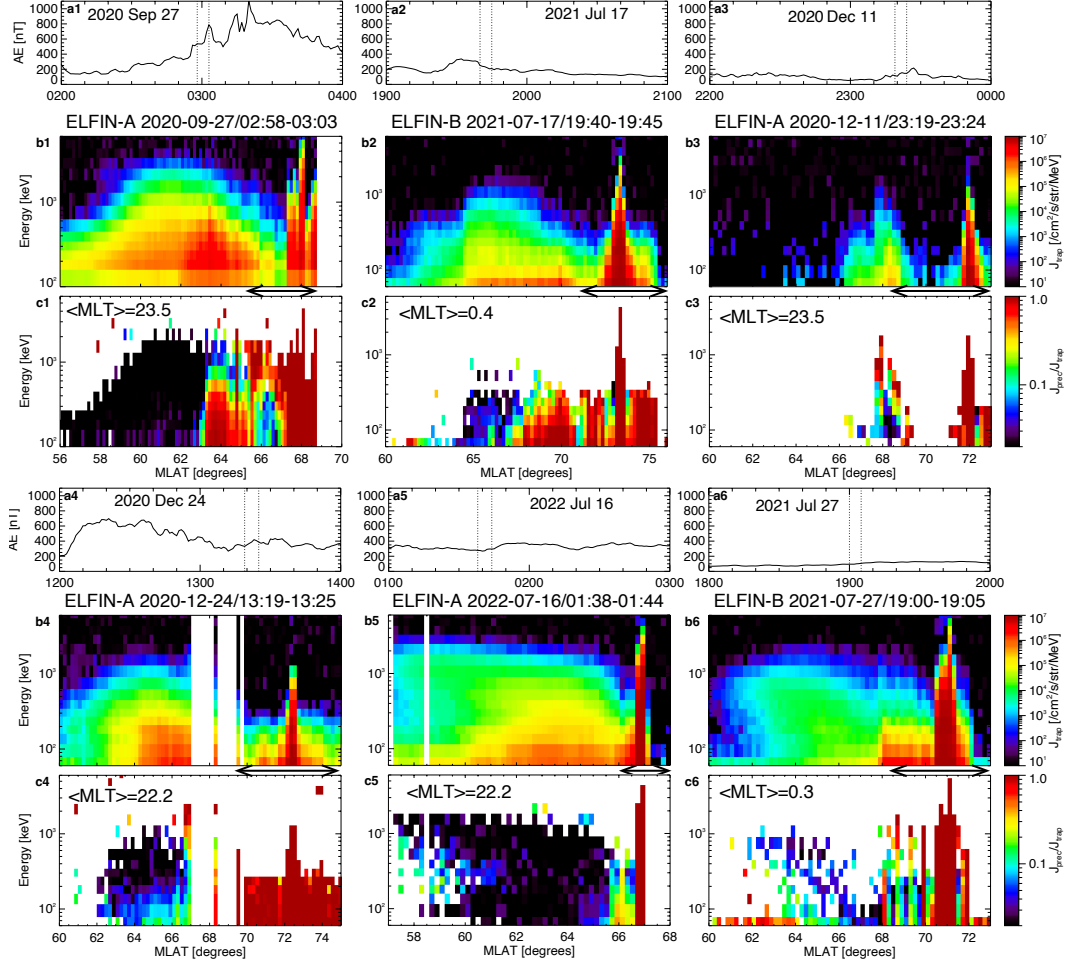


Figure 2. Overview of six ELFIN events with relativistic electron observations in near-Earth magnetotail: on 27 September 2020 at 03:02UT, 17 July 2021 at 19:45 UT, 11 December 2020 at 23:20UT, 24 December 2020 at 13:23UT, 16 July 2021 at 19:05UT, and 27 July 2021 at 01:42UT. For each event, we show (a) the AE index during the 2h interval embedding ELFIN observations, and ELFIN measurements of (b) locally trapped fluxes and (c) precipitating-to-trapped flux ratio. Black arrows mark the plasma sheet region during each orbit.

cellent telemetry with data available from almost each orbit ($\sim 90\text{min}$), (2) high energy resolution and sensitivity, allowing for a reliable measurement of the spectrum of relativistic electron bursts.

Figure 3(a) shows CIRBE observations of an relativistic burst event: the peak of relativistic electron fluxes ($\sim 64.5^\circ$ magnetic latitude) is well separated from the outer radiation belt region (see the black contour lines). Note that in the absence of measurements of $< 250\text{keV}$ electron fluxes (i.e., the dominant energetic electron population in the plasma sheet, see Artemyev et al., 2022), the relativistic electron burst measured by CIRBE was not embedded into the much more extended plasma sheet, unlike ELFIN observations. Therefore, in CIRBE data, the relativistic electron bursts in the magnetotail are not as vibrant compared to the outer radiation belt fluxes, and we mark them with red arrows.

The event in Fig. 3(a) was in conjunction with POES NOAA-19 observations: Fig. 3(b) shows that the relativistic burst occurred well poleward of the electron isotropy boundary (at $\sim 62.5^\circ$ magnetic latitude), as implied from the precipitating and trapped electron ($> 30\text{keV}$) fluxes at POES (we use AACGM magnetic latitudes for both CIRBE and POES, see Heres & Bonito, 2007). This relativistic electron burst was observed when THEMIS E (Angelopoulos, 2008) was in the night-side magnetosphere and detected enhanced energetic electron fluxes. Panels (d-f) show magnetic field perturbations (Auster et al., 2008), plasma flow speed (McFadden et al., 2008), and energetic electron fluxes (Angelopoulos, Sibeck, et al., 2008). The interval delineated by the vertical dashed lines correspond to near-equatorial measurements (implied by the $|B_x|$ decrease) following a plasma injection around 15:30 UT (better seen in THEMIS A and D; not shown). This injection results in a magnetotail dipolarization ($|B_x|$ decreases, B_z increases) and energetic flux enhancement. Therefore, CIRBE observations are associated with substorm activity (panel (c) shows the AE index increase around 17:00 UT), similar to ELFIN observations shown in Figs. 1, 2. Also, similar to the ELFIN/MMS comparison, THEMIS does not detect an increase in relativistic electron fluxes (the main flux increase is below 500keV). However, a comparison of $< 500\text{keV}$ energy spectra measured by CIRBE and THEMIS shows a strong similarity (see Fig. 3(g)), confirming CIRBE's projection to the post-injection magnetotail, close to the location of THEMIS E. Despite several independent confirmations that the CIRBE measurements at $\text{MLAT} < -64^\circ$ originate from the plasma sheet—such as their location relative to the isotropy boundary observed by POES and spectrum validation with THEMIS—we cannot definitively pinpoint the location of the relativistic bursts detected by CIRBE without direct measurements of precipitating flux. These bursts could potentially still represent the poleward edge of the outer radiation belt. Therefore, systematic analysis of more events of this kind is necessary to better understand their true nature.

The energy spectrum of the relativistic electron burst in Fig. 3(g) exhibits a power-law shape, in contrast to a clear exponential shape within the outer radiation belt. Fitting to the function that combines power-law and exponential components: $A \cdot E^{-\alpha} \cdot \exp(-E/E_0)$, we derive values for the mean energy E_0 and power-law index α . For the magnetotail, we find $E_0 \approx 400\text{keV}$ (i.e., the exponential factor $\sim \exp(-E/E_0)$ exerts a negligible influence on the spectrum at $< 2\text{MeV}$) and $\alpha \approx 4$; on the other hand, for the outer radiation belt, we have $E_0 \approx 130\text{keV}$ (indicating a pronounced exponential decay at high energies), $\alpha \approx 0$. Thus, there is a distinct difference between the exponential spectrum in the outer radiation belt (characterized by the mean energy E_0 of the exponential decay, $\sim \exp(-E/E_0)$) and the power-law spectrum in the magnetotail relativistic burst (dictated by the index α). This power-law spectrum is typical for such relativistic populations: Fig. 4 shows six more examples of substorm-associated relativistic electron bursts with such power-law spectra. In all events, the relativistic bursts are observed poleward of the outer radiation belt (the boundary between the outer radiation belt and the magnetotail can be discerned from measurements at a nearby POES

satellite, as seen in the precipitating and trapped fluxes of $> 30\text{keV}$ electrons), with energies exceeding 1MeV . The typical power-law index α for these events varies within the $[1.5, 4.5]$ range, with $E_0 > 500\text{keV}$ making the factor $\sim \exp(-E/E_0)$ insignificant for $< 2\text{MeV}$ energies. The power-law spectrum with the exponential cut-off is expected for electron acceleration in a single reconnection region (see details in Bulanov & Sasorov, 1976; Burkhart et al., 1990; Birn et al., 2012), whereas multiple (turbulent) reconnection would produce a power-law energy tail (Hoshino, 2012; Johnson et al., 2022; Oka et al., 2022). Thus, we suggest that the observed relativistic electron populations were initially accelerated in near-Earth turbulent reconnection region (distributions observed around the near-Earth reconnection region usually show upper energies at $\sim 100\text{keV}$, see Ashour-Abdalla et al., 2011; Zhou et al., 2011; Birn et al., 2013; Usanova & Ergun, 2022), and then adiabatically or quasi-adiabatically heated during Earthward injection. Conservation of the first adiabatic moment has been shown to provide a factor of $\times 10$ in energy for near-Earth injections (see Birn et al., 2014; Sorathia et al., 2018; Eshetu et al., 2019) and will likely play an important role for any Earthward motion. However, since the observed electrons precipitate tailward from the injection region, conservation of the second adiabatic moment as field lines contract may also play an important role. It is well known that field lines in contracting flux ropes can energize particles through Fermi acceleration and create power-laws (see Arnold et al., 2021; Li et al., 2021; Q. Zhang et al., 2021; Nakanotani et al., 2022). In the magnetotail a similar process is likely at play from particles mirroring off the near-Earth magnetic field on flux ropes associated with fast flows that are contracting and moving Earthward. This combination may potentially explain the observed relativistic electron bursts at $\sim 1\text{MeV}$ (see also discussion in Turner, Cohen, Michael, et al., 2021), which still requires detailed quantification, especially for the more extreme events reaching $\sim 5\text{MeV}$ in Fig. 2.

4 Conclusions

In this study, we have analyzed relativistic and super-relativistic electron events in near-Earth magnetotail captured by low-altitude CubeSats. These bursts of relativistic electrons exhibit the following properties:

- Electron energies within these bursts can reach the relativistic ($\sim 1\text{MeV}$) and even ultra-relativistic ($\sim 3\text{MeV}$) range
- These bursts are well separated from the outer radiation belt and are thus likely related to acceleration mechanisms in the magnetotail.
- These are spatially and temporally localized bursts.
- Observed poleward from the electron isotropy boundary, these bursts are likely associated with an isotropic (highly scattered) electron population, indicative of relativistic electron precipitation into the polar cap.

Earth's magnetotail is a spatially compact system dominated by thermal electron energies below $\sim 1\text{keV}$ (e.g., Artemyev et al., 2012). Effective acceleration mechanisms are thus required to explain the observed relativistic electron population. Magnetic field line reconnection in the magnetotail current sheet alone may not produce these electrons (see theoretical estimates Bulanov & Sasorov, 1976; Burkhart et al., 1990; Birn et al., 2012; Egedal et al., 2012), but it can generate the *seed* electron population at $\sim 10 - 100\text{keV}$ (see Turner, Cohen, Bingham, et al., 2021, and references therein), which can be further adiabatically accelerated during Earthward transport (Ashour-Abdalla et al., 2011, 2013; Pan et al., 2012). Although electrons of such energies are not magnetized in the magnetotail and do not preserve their adiabatic invariants, these demagnetized electrons can still experience adiabatic acceleration with energy scaled with the equatorial magnetic field intensity, $\propto B_{eq}^\kappa$ (the power-law exponent, $\kappa < 1$, depends on the specific magnetic field configuration, see details in Zelenyi et al., 2013, and references therein). Therefore, the presented observations (along with historical datasets collected by ISEE-

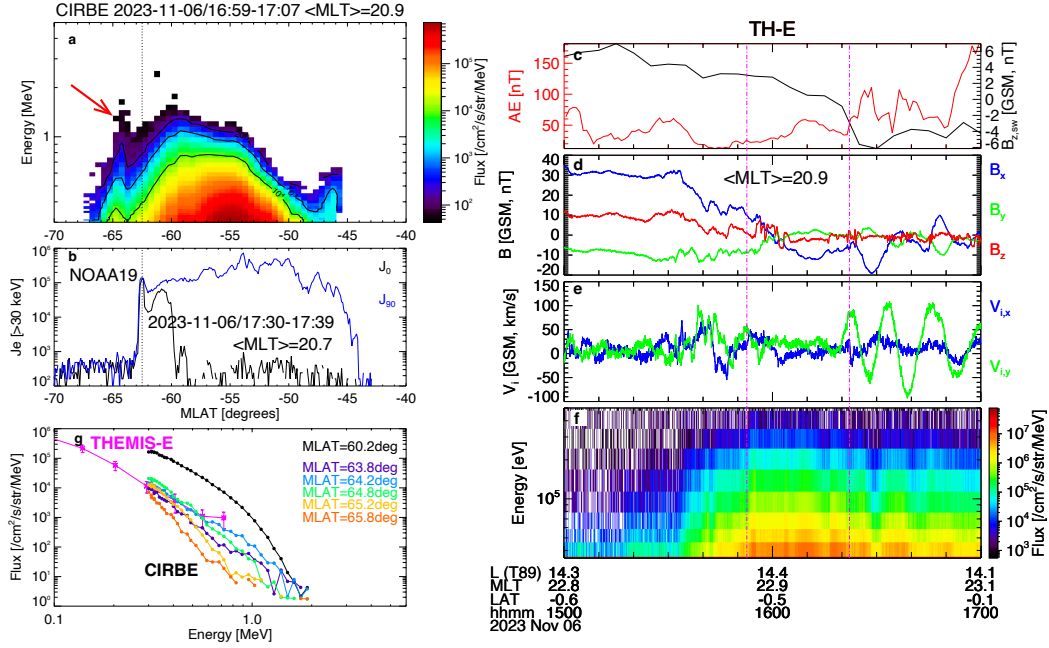


Figure 3. Overview of one CIRBE event with relativistic electron observations in near-Earth magnetotail on 06 November 2023, at $\sim 17:05$ UT. Panel (a) shows locally trapped electron fluxes (versus magnetic latitude). Panel (b) shows POES observations of trapped and precipitating fluxes of $> 30\text{keV}$ electrons (vertical dashed line shows electron isotropy boundary). Panel (c) shows the AE index and solar wind B_z for the 2h interval embedding the CIRBE event. Panels (d,e,f) show THEMIS observations in the magnetotail: GSM magnetic field from (Auster et al., 2008), GSM plasma flows from (McFadden et al., 2008), and energetic electron spectra from (Angelopoulos, Sibeck, et al., 2008). Panel (g) shows the 1D electron spectra measured by CIRBE during relativistic electron bursts in the magnetotail, in comparison with THEMIS measurements during the substorm injection.

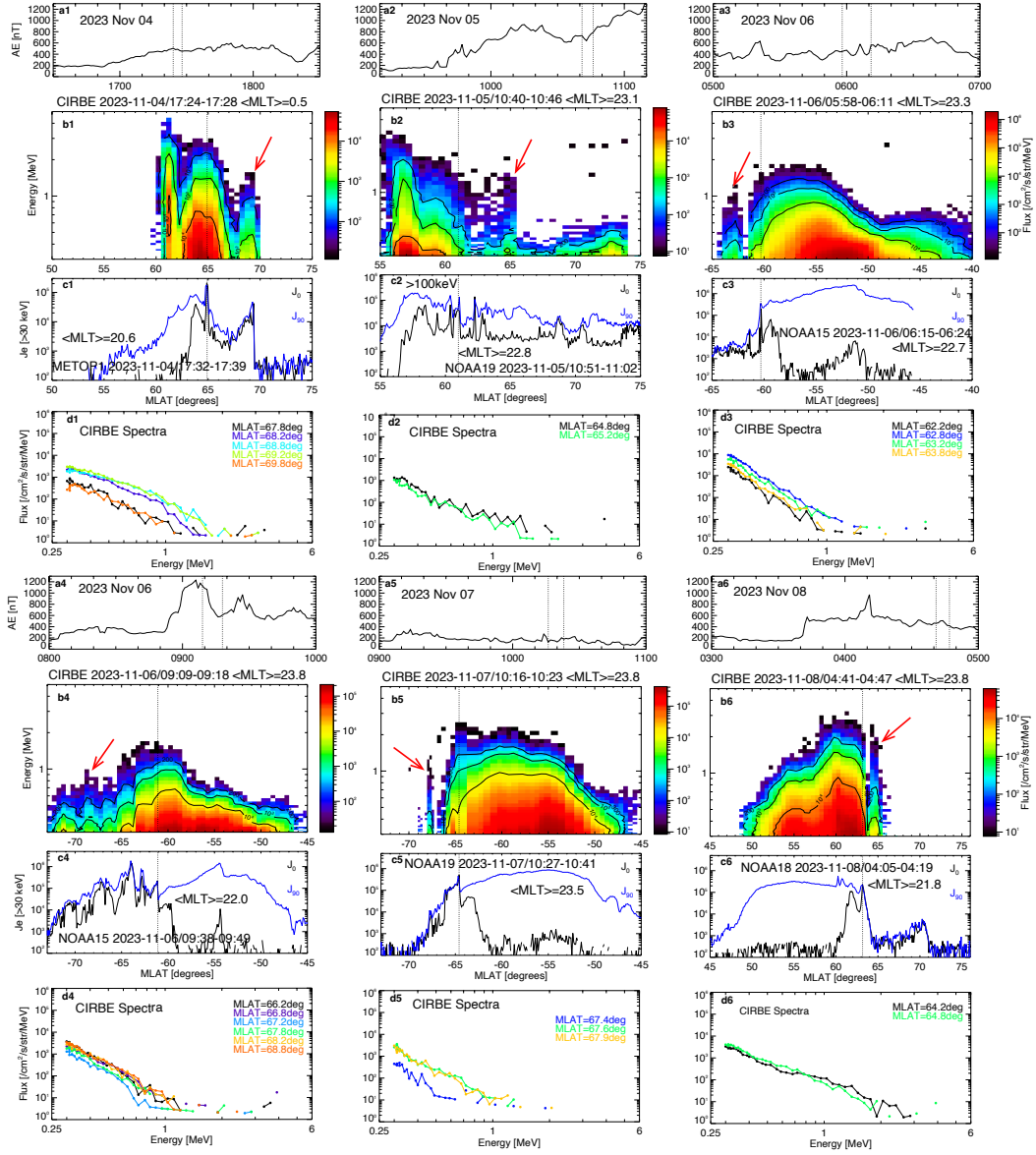


Figure 4. Overview of six CIRBE events with relativistic electron observations in near-Earth magnetotail: 4 November 2023, at 17:30UT; 4 November 2023, at 19:30UT; 5 November 202, at 10:40UT, 6 November 2023, at 06:00UT; 6 November 2023, at 09:20UT; and 7 November 2023, at 10:20UT. For each event, we show (a) AE index during the 2h interval embedding CIRBE observations, (b) CIRBE measurements of locally trapped fluxes, (c) POES measurements of trapped and precipitating fluxes of > 30 keV electrons, and (d) the 1D electron spectra measured by CIRBE during relativistic electron bursts in the magnetotail.

3 and Imp 8; see Baker & Stone, 1977; Slavin et al., 1992; Richardson et al., 1993) demonstrate the potential for producing relativistic ($\geq 1\text{MeV}$) electrons within the plasma systems of spatial scales $\leq 10^2\rho_e$: the diameter of Earth’s magnetotail is $\sim 40R_E$, which is smaller than 100 times the electron gyroradii (ρ_e) at $\geq 1\text{MeV}$ and $\sim 1\text{nT}$ equatorial field. This makes the magnetotail (and the magnetic reconnection region) an extremely efficient yet compact accelerator. These observations, along with the future developed acceleration models and resolving the question of plasma sheet ($\sim 1\text{keV}$) electron pre-acceleration up to 50–100 keV before undergoing adiabatic acceleration to 1MeV, may be very important, because magnetic reconnection is responsible for the transformation of magnetic field energy into plasma heating and charged particle acceleration in a wide range of space plasma systems (e.g., Zweibel & Yamada, 2009; Hoshino & Lyubarsky, 2012; Ji et al., 2022; Guo et al., 2024, and references therein).

Acknowledgments

We acknowledge the CIRBE mission team for their efforts in making the dataset accessible to the community, under NASA Heliophysics Division Grants 80NSSC19K0995 and 80NSSC21K0583. We are grateful to NASA’s CubeSat Launch Initiative for ELFIN’s successful launch in the desired orbits. We acknowledge early support of ELFIN project by the AFOSR, under its University Nanosat Program, UNP-8 project, contract FA9453-12-D-0285, and by the California Space Grant program. We acknowledge critical contributions by numerous ELFIN team members and support by NASA 80NSSC22K1005 and NSF grants AGS-1242918, AGS-2019950. We acknowledge NASA contract NAS5-02099 for the use of data from the THEMIS Mission. We thank the entire MMS team and instrument leads for data access and support.

A.V.A and X.-J. Z. acknowledge support from the NASA grants 80NSSC23K0108, 80NSSC23K0413, 80NSSC24K0561. X.-J. Z. acknowledges support from the NASA grant 80NSSC24K0138 and the NSF grant 2329897. V.A. acknowledges support by NSF award AGS-2019950 and NASA contract NAS5-02099. M.S. was supported by the MMS via subcontract to the SwRI (NNG04EB99C).

Open Research

Fluxes measured by ELFIN are available in ELFIN data archive <https://data.elfin.ucla.edu/> in CDF format.

Fluxes measured by CIRBE are available in CIRBE data archive <https://lasp.colorado.edu/cirbe/data-products/> in NCDF format.

THEMIS and MMS data are available at <http://themis.ssl.berkeley.edu> and <https://lasp.colorado.edu/mms>.

Data analysis was done using SPEDAS V4.1 (Angelopoulos et al., 2019). The software can be downloaded from http://spedas.org/wiki/index.php?title=Downloads_and_Installation.

References

- Angelopoulos, V. (2008, December). The THEMIS Mission. *Space Sci. Rev.*, *141*, 5–34. doi: 10.1007/s11214-008-9336-1
- Angelopoulos, V., Artemyev, A., Phan, T. D., & Miyashita, Y. (2020, January). Near-Earth magnetotail reconnection powers space storms. *Nature Physics*, *16*(3), 317–321. doi: 10.1038/s41567-019-0749-4
- Angelopoulos, V., Cruce, P., Drozdov, A., Grimes, E. W., Hatzigeorgiu, N., King, D. A., ... Schroeder, P. (2019, January). The Space Physics Environment Data Analysis System (SPEDAS). *Space Sci. Rev.*, *215*, 9. doi: 10.1007/s11214-018-0576-4
- Angelopoulos, V., McFadden, J. P., Larson, D., Carlson, C. W., Mende, S. B., Frey,

- H., ... Kepko, L. (2008, August). Tail Reconnection Triggering Substorm Onset. *Science*, *321*, 931-935. doi: 10.1126/science.1160495
- Angelopoulos, V., Sibeck, D., Carlson, C. W., McFadden, J. P., Larson, D., Lin, R. P., ... Sigwarth, J. (2008, December). First Results from the THEMIS Mission. *Space Sci. Rev.*, *141*, 453-476. doi: 10.1007/s11214-008-9378-4
- Angelopoulos, V., Tsai, E., Bingley, L., Shaffer, C., Turner, D. L., Runov, A., ... Zhang, G. Y. (2020, July). The ELFING Mission. *Space Sci. Rev.*, *216*(5), 103. doi: 10.1007/s11214-020-00721-7
- Angelopoulos, V., Zhang, X. J., Artemyev, A. V., Mourenas, D., Tsai, E., Wilkins, C., ... Zarifian, A. (2023, August). Energetic Electron Precipitation Driven by Electromagnetic Ion Cyclotron Waves from ELFING's Low Altitude Perspective. *Space Sci. Rev.*, *219*(5), 37. doi: 10.1007/s11214-023-00984-w
- Arnold, H., Drake, J. F., Swisdak, M., Guo, F., Dahlin, J. T., Chen, B., ... Shen, C. (2021, April). Electron Acceleration during Macroscale Magnetic Reconnection. *Phys. Rev. Lett.*, *126*(13), 135101. doi: 10.1103/PhysRevLett.126.135101
- Artemyev, A. V., Angelopoulos, V., Zhang, X. J., Runov, A., Petrukovich, A., Nakamura, R., ... Wilkins, C. (2022, October). Thinning of the Magnetotail Current Sheet Inferred From Low-Altitude Observations of Energetic Electrons. *Journal of Geophysical Research (Space Physics)*, *127*(10), e2022JA030705. doi: 10.1029/2022JA030705
- Artemyev, A. V., Petrukovich, A. A., Nakamura, R., & Zelenyi, L. M. (2012). Adiabatic electron heating in the magnetotail current sheet: Cluster observations and analytical models. *J. Geophys. Res.*, *117*, A06219. doi: 10.1029/2012JA017513
- Ashour-Abdalla, M., El-Alaoui, M., Goldstein, M. L., Zhou, M., Schriver, D., Richard, R., ... Hwang, K.-J. (2011, April). Observations and simulations of non-local acceleration of electrons in magnetotail magnetic reconnection events. *Nature Physics*, *7*, 360-365. doi: 10.1038/nphys1903
- Ashour-Abdalla, M., Schriver, D., Alaoui, M. E., Richard, R., Walker, R., Goldstein, M. L., ... Zhou, M. (2013, August). Direct auroral precipitation from the magnetotail during substorms. *Geophys. Res. Lett.*, *40*(15), 3787-3792. doi: 10.1002/grl.50635
- Auster, H. U., Glassmeier, K. H., Magnes, W., Aydogar, O., Baumjohann, W., Constantinescu, D., ... Wiedemann, M. (2008, December). The THEMIS Fluxgate Magnetometer. *Space Sci. Rev.*, *141*, 235-264. doi: 10.1007/s11214-008-9365-9
- Baker, D. N., Pulkkinen, T. I., Angelopoulos, V., Baumjohann, W., & McPherron, R. L. (1996, June). Neutral line model of substorms: Past results and present view. *J. Geophys. Res.*, *101*, 12975-13010. doi: 10.1029/95JA03753
- Baker, D. N., & Stone, E. C. (1977, April). Observations of energetic electrons ($E \gtrsim 200$ keV) in the Earth's magnetotail: Plasma sheet and Fireball observations. *J. Geophys. Res.*, *82*(10), 1532. doi: 10.1029/JA082i010p01532
- Birn, J., Artemyev, A. V., Baker, D. N., Echim, M., Hoshino, M., & Zelenyi, L. M. (2012). Particle acceleration in the magnetotail and aurora. *Space Sci. Rev.*, *173*, 49-102. doi: 10.1007/s11214-012-9874-4
- Birn, J., Hesse, M., Nakamura, R., & Zaharia, S. (2013, May). Particle acceleration in dipolarization events. *J. Geophys. Res.*, *118*, 1960-1971. doi: 10.1002/jgra.50132
- Birn, J., Runov, A., & Hesse, M. (2014, May). Energetic electrons in dipolarization events: Spatial properties and anisotropy. *Journal of Geophysical Research (Space Physics)*, *119*(5), 3604-3616. doi: 10.1002/2013JA019738
- Birn, J., Thomsen, M. F., & Hesse, M. (2004, May). Electron acceleration in the dynamic magnetotail: Test particle orbits in three-dimensional magnetohydrodynamic simulation fields. *Physics of Plasmas*, *11*, 1825-1833. doi:

10.1063/1.1704641

- Blake, J. B., Mauk, B. H., Baker, D. N., Carranza, P., Clemmons, J. H., Craft, J., ... Westlake, J. (2016, March). The Fly's Eye Energetic Particle Spectrometer (FEEPS) Sensors for the Magnetospheric Multiscale (MMS) Mission. *Space Sci. Rev.*, *199*, 309-329. doi: 10.1007/s11214-015-0163-x
- Bulanov, S. V., & Sasorov, P. V. (1976, February). Energy spectrum of particles accelerated in the neighborhood of a line of zero magnetic field. *Soviet Astronomy*, *19*, 464-468.
- Burch, J. L., Moore, T. E., Torbert, R. B., & Giles, B. L. (2016, March). Magnetospheric Multiscale Overview and Science Objectives. *Space Sci. Rev.*, *199*, 5-21. doi: 10.1007/s11214-015-0164-9
- Burkhart, G. R., Drake, J. F., & Chen, J. (1990, November). Magnetic reconnection in collisionless plasmas - Prescribed fields. *J. Geophys. Res.*, *95*, 18833-18848. doi: 10.1029/JA095iA11p18833
- Cohen, I. J., Turner, D. L., Mauk, B. H., Bingham, S. T., Blake, J. B., Fennell, J. F., & Burch, J. L. (2021, January). Characteristics of Energetic Electrons Near Active Magnetotail Reconnection Sites: Statistical Evidence for Local Energization. *Geophys. Res. Lett.*, *48*(1), e90087. doi: 10.1029/2020GL090087
- Egedal, J., Daughton, W., & Le, A. (2012, April). Large-scale electron acceleration by parallel electric fields during magnetic reconnection. *Nature Physics*, *8*, 321-324. doi: 10.1038/nphys2249
- Ergun, R. E., Ahmadi, N., Kromyda, L., Schwartz, S. J., Chasapis, A., Hoilijoki, S., ... Giles, B. L. (2020, August). Observations of Particle Acceleration in Magnetic Reconnection-driven Turbulence. *Astrophys. J.*, *898*(2), 154. doi: 10.3847/1538-4357/ab9ab6
- Eshetu, W. W., Lyon, J. G., Hudson, M. K., & Wiltberger, M. J. (2019, February). Simulations of Electron Energization and Injection by BBFs Using High-Resolution LFM MHD Fields. *Journal of Geophysical Research (Space Physics)*, *124*(2), 1222-1238. doi: 10.1029/2018JA025789
- Evans, D. S., & Greer, M. S. (2004). *Polar orbiting environmental satellite space environment monitor-2: instrument description and archive data documentation*.
- Fu, H. S., Khotyaintsev, Y. V., Vaivads, A., Retinò, A., & André, M. (2013, July). Energetic electron acceleration by unsteady magnetic reconnection. *Nature Physics*, *9*, 426-430. doi: 10.1038/nphys2664
- Fu, H. S., Xu, Y., Vaivads, A., & Khotyaintsev, Y. V. (2019, January). Super-efficient Electron Acceleration by an Isolated Magnetic Reconnection. *Astrophys. J. Lett.*, *870*(2), L22. doi: 10.3847/2041-8213/aafa75
- Gabrielse, C., Spanswick, E., Artemyev, A., Nishimura, Y., Runov, A., Lyons, L., ... Donovan, E. (2019, Jul). Utilizing the Heliophysics/Geospace System Observatory to Understand Particle Injections: Their Scale Sizes and Propagation Directions. *Journal of Geophysical Research (Space Physics)*, *124*(7), 5584-5609. doi: 10.1029/2018JA025588
- Gonzalez, W., & Parker, E. (2016). *Magnetic Reconnection* (Vol. 427). doi: 10.1007/978-3-319-26432-5
- Guo, F., Liu, Y.-H., Zenitani, S., & Hoshino, M. (2024, June). Magnetic Reconnection and Associated Particle Acceleration in High-Energy Astrophysics. *Space Sci. Rev.*, *220*(4), 43. doi: 10.1007/s11214-024-01073-2
- Heres, W., & Bonito, N. A. (2007). *Alternative method of computing altitude adjustment corrected geomagnetic coordinates as applied to igrf epoch 2005* (Tech. Rep. No. Scientific Report AFRL-RV-HA-TR-2007-1190). Retrieved from https://www.aer.com/siteassets/resources/aacgm_heres_2007.pdf
- Hoshino, M. (2012, March). Stochastic Particle Acceleration in Multiple Magnetic Islands during Reconnection. *Physical Review Letters*, *108*(13), 135003. doi: 10.1103/PhysRevLett.108.135003

- Hoshino, M., & Lyubarsky, Y. (2012, November). Relativistic Reconnection and Particle Acceleration. *Space Sci. Rev.*, *173*, 521-533. doi: 10.1007/s11214-012-9931-z
- Hua, M., Bortnik, J., Spence, H. E., & Reeves, G. D. (2023, April). Testing the key processes that accelerate outer radiation belt relativistic electrons during geomagnetic storms. *Frontiers in Astronomy and Space Sciences*, *10*, 1168636. doi: 10.3389/fspas.2023.1168636
- Huang, S. Y., Vaivads, A., Khotyaintsev, Y. V., Zhou, M., Fu, H. S., Retinò, A., ... Pang, Y. (2012, June). Electron acceleration in the reconnection diffusion region: Cluster observations. *Geophys. Res. Lett.*, *39*(11), L11103. doi: 10.1029/2012GL051946
- Imada, S., Nakamura, R., Daly, P. W., Hoshino, M., Baumjohann, W., Mühlbachler, S., ... Rème, H. (2007, March). Energetic electron acceleration in the downstream reconnection outflow region. *J. Geophys. Res.*, *112*, 3202. doi: 10.1029/2006JA011847
- Ji, H., Daughton, W., Jara-Almonte, J., Le, A., Stanier, A., & Yoo, J. (2022, February). Magnetic reconnection in the era of exascale computing and multiscale experiments. *Nature Reviews Physics*, *4*(4), 263-282. doi: 10.1038/s42254-021-00419-x
- Johnson, G., Kilian, P., Guo, F., & Li, X. (2022, July). Particle Acceleration in Magnetic Reconnection with Ad Hoc Pitch-angle Scattering. *Astrophys. J.*, *933*(1), 73. doi: 10.3847/1538-4357/ac7143
- Jun, C.-W., Miyoshi, Y., Kurita, S., Yue, C., Bortnik, J., Lyons, L., ... Shinohara, I. (2021, June). The Characteristics of EMIC Waves in the Magnetosphere Based on the Van Allen Probes and Arase Observations. *Journal of Geophysical Research (Space Physics)*, *126*(6), e29001. doi: 10.1029/2020JA029001
- Khoo, L.-Y., Li, X., Selesnick, R., Schiller, Q., Zhang, K., Zhao, H., ... others (2022). On the challenges of measuring energetic particles in the inner belt: A geant4 simulation of an energetic particle detector instrument, reptile-2. *Journal of Geophysical Research: Space Physics*, *127*(4), e2021JA030249.
- Kim, H.-J., Noh, S. J., Lee, D. Y., Lyons, L., Bortnik, J., Nagai, T., ... Hua, M. (2023, March). Can strong substorm-associated MeV electron injections be an important cause of large radiation belt enhancements? *Frontiers in Astronomy and Space Sciences*, *10*, 55. doi: 10.3389/fspas.2023.1128923
- Li, X. (2024). Unveiling energetic particle dynamics in the near-earth environment from cubesat missions. *AGU Advances*, *5*(3), e2024AV001256. doi: 10.1029/2024AV001256
- Li, X., Guo, F., & Liu, Y.-H. (2021, May). The acceleration of charged particles and formation of power-law energy spectra in nonrelativistic magnetic reconnection. *Physics of Plasmas*, *28*(5), 052905. doi: 10.1063/5.0047644
- Li, X., Kohnert, R., Palo, S., Selesnick, R., Khoo, L., & Schiller, Q. (2022). Two generations of CubeSat missions (CSSWE and CIRBE) to take on the challenges of measuring relativistic electrons in Earth's magnetosphere. In *In 36th annual small satellite conference*. Retrieved from [Retrievedfromhttps://digitalcommons.usu.edu/cgi/viewcontent.cgi?article=5311&context=smallsat](https://digitalcommons.usu.edu/cgi/viewcontent.cgi?article=5311&context=smallsat)
- Li, X., Selesnick, R., Mei, Y., O'Brien, D., Hogan, B., Xiang, Z., ... Baker, D. N. (2024). First results from reptile-2 measurements onboard cirbe. *Geophysical Research Letters*, *51*(3), e2023GL107521. doi: 10.1029/2023GL107521
- Lin, Y., Wang, X. Y., Fok, M. C., Buzulukova, N., Perez, J. D., Cheng, L., & Chen, L. J. (2021, March). Magnetotail Inner Magnetosphere Transport Associated With Fast Flows Based on Combined Global Hybrid and CIMI Simulation. *Journal of Geophysical Research (Space Physics)*, *126*(3), e28405. doi: 10.1029/2020JA028405
- McFadden, J. P., Carlson, C. W., Larson, D., Ludlam, M., Abiad, R., Elliott, B.,

- ... Angelopoulos, V. (2008, December). The THEMIS ESA Plasma Instrument and In-flight Calibration. *Space Sci. Rev.*, *141*, 277-302. doi: 10.1007/s11214-008-9440-2
- Mourenas, D., Artemyev, A. V., Zhang, X. J., Angelopoulos, V., Tsai, E., & Wilkins, C. (2021, November). Electron Lifetimes and Diffusion Rates Inferred From ELFIN Measurements at Low Altitude: First Results. *Journal of Geophysical Research (Space Physics)*, *126*(11), e29757. doi: 10.1029/2021JA029757
- Nakamura, R., Baumjohann, W., Klecker, B., Bogdanova, Y., Balogh, A., Rème, H., ... Runov, A. (2002, October). Motion of the dipolarization front during a flow burst event observed by Cluster. *Geophys. Res. Lett.*, *29*(20), 20000-1. doi: 10.1029/2002GL015763
- Nakanotani, M., Zank, G. P., & Zhao, L. (2022, August). Particle acceleration in an MHD-scale system of multiple current sheets. *Frontiers in Astronomy and Space Sciences*, *9*, 954040. doi: 10.3389/fspas.2022.954040
- Øieroset, M., Lin, R. P., Phan, T. D., Larson, D. E., & Bale, S. D. (2002, October). Evidence for Electron Acceleration up to ~ 300 keV in the Magnetic Reconnection Diffusion Region of Earth's Magnetotail. *Physical Review Letters*, *89*(19), 195001. doi: 10.1103/PhysRevLett.89.195001
- Oka, M., Phan, T., Øieroset, M., Turner, D., Drake, J., Li, X., ... Burch, J. (2022, May). Electron energization and thermal to non-thermal energy partition during earth's magnetotail reconnection. *Physics of Plasmas*, *29*(5), 052904. doi: 10.1063/5.0085647
- Pan, Q., Ashour-Abdalla, M., El-Alaoui, M., Walker, R. J., & Goldstein, M. L. (2012, December). Adiabatic acceleration of suprathermal electrons associated with dipolarization fronts. *J. Geophys. Res.*, *117*, 12224. doi: 10.1029/2012JA018156
- Paschmann, G., Øieroset, M., & Phan, T. (2013, October). In-Situ Observations of Reconnection in Space. *Space Sci. Rev.*, *178*, 385-417. doi: 10.1007/s11214-012-9957-2
- Retinò, A., Nakamura, R., Vaivads, A., Khotyaintsev, Y., Hayakawa, T., Tanaka, K., ... Cornilleau-Wehrin, N. (2008, December). Cluster observations of energetic electrons and electromagnetic fields within a reconnecting thin current sheet in the Earth's magnetotail. *J. Geophys. Res.*, *113*, 12215. doi: 10.1029/2008JA013511
- Richardson, I. G., Owen, C. J., Slavin, J. A., & von Rosenvinge, T. T. (1993, August). Energetic (>0.2 MeV) electron bursts observed by ISEE 3 in the deep ($>240 R_E$) geomagnetic tail. *J. Geophys. Res.*, *98*(A8), 13441-13452. doi: 10.1029/93JA00501
- Runov, A., Angelopoulos, V., Sitnov, M. I., Sergeev, V. A., Bonnell, J., McFadden, J. P., ... Auster, U. (2009, July). THEMIS observations of an earthward-propagating dipolarization front. *Geophys. Res. Lett.*, *36*, L14106. doi: 10.1029/2009GL038980
- Russell, C. T., Anderson, B. J., Baumjohann, W., Bromund, K. R., Dearborn, D., Fischer, D., ... Richter, I. (2016, March). The Magnetospheric Multiscale Magnetometers. *Space Sci. Rev.*, *199*, 189-256. doi: 10.1007/s11214-014-0057-3
- Sergeev, V. A., Nishimura, Y., Kubyshkina, M., Angelopoulos, V., Nakamura, R., & Singer, H. (2012, January). Magnetospheric location of the equatorward prebreakup arc. *Journal of Geophysical Research (Space Physics)*, *117*(A1), A01212. doi: 10.1029/2011JA017154
- Sitnov, M. I., Birn, J., Ferdousi, B., Gordeev, E., Khotyaintsev, Y., Merkin, V., ... Zhou, X. (2019, Jun). Explosive Magnetotail Activity. *Space Sci. Rev.*, *215*(4), 31. doi: 10.1007/s11214-019-0599-5
- Sitnov, M. I., Swisdak, M., & Divin, A. V. (2009, April). Dipolarization fronts as a

- signature of transient reconnection in the magnetotail. *J. Geophys. Res.*, *114*, A04202. doi: 10.1029/2008JA013980
- Slavin, J. A., Smith, M. F., Mazur, E. L., Baker, D. N., Iyemori, T., Singer, H. J., & Greenstadt, E. W. (1992, April). ISEE 3 plasmoid and TCR observations during an extended interval of substorm activity. *Geophys. Res. Lett.*, *19*(8), 825-828. doi: 10.1029/92GL00394
- Sorathia, K. A., Ukhorskiy, A. Y., Merkin, V. G., Fennell, J. F., & Claudepierre, S. G. (2018, July). Modeling the Depletion and Recovery of the Outer Radiation Belt During a Geomagnetic Storm: Combined MHD and Test Particle Simulations. *Journal of Geophysical Research (Space Physics)*, *123*(7), 5590-5609. doi: 10.1029/2018JA025506
- Tsai, E., & et al. (2024). Remote Sensing of Electron Precipitation Mechanisms Enabled by ELFIN Mission Operations and ADCS Design. *Engineering Archive*. doi: 10.31224/3487
- Turner, D. L., Cohen, I. J., Bingham, S. T., Stephens, G. K., Sitnov, M. I., Mauk, B. H., ... Burch, J. L. (2021, January). Characteristics of Energetic Electrons Near Active Magnetotail Reconnection Sites: Tracers of a Complex Magnetic Topology and Evidence of Localized Acceleration. *Geophys. Res. Lett.*, *48*(2), e90089. doi: 10.1029/2020GL090089
- Turner, D. L., Cohen, I. J., Michael, A., Sorathia, K., Merkin, S., Mauk, B. H., ... Reeves, G. D. (2021, November). Can Earth's Magnetotail Plasma Sheet Produce a Source of Relativistic Electrons for the Radiation Belts? *Geophys. Res. Lett.*, *48*(21), e95495. doi: 10.1029/2021GL095495
- Usanova, M. E., & Ergun, R. E. (2022, July). Electron Energization by High-Amplitude Turbulent Electric Fields: A Possible Source of the Outer Radiation Belt. *Journal of Geophysical Research (Space Physics)*, *127*(7), e30336. doi: 10.1029/2022JA030336
- Vaivads, A., Retinò, A., Khotyaintsev, Y. V., & André, M. (2011, October). Suprathermal electron acceleration during reconnection onset in the magnetotail. *Annales Geophysicae*, *29*, 1917-1925. doi: 10.5194/angeo-29-1917-2011
- Wilken, B., Daly, P. W., Mall, U., Aarsnes, K., Baker, D. N., Belian, R. D., ... Zong, Q.-G. (2001, October). First results from the RAPID imaging energetic particle spectrometer on board Cluster. *Annales Geophysicae*, *19*, 1355-1366. doi: 10.5194/angeo-19-1355-2001
- Wilkins, C., Angelopoulos, V., Runov, A., Artemyev, A., Zhang, X. J., Liu, J., & Tsai, E. (2023, October). Statistical Characteristics of the Electron Isotropy Boundary. *Journal of Geophysical Research (Space Physics)*, *128*(10), e2023JA031774. doi: 10.1029/2023JA031774
- Young, D. T., Burch, J. L., Gomez, R. G., De Los Santos, A., Miller, G. P., Wilson, P., ... Webster, J. M. (2016, December). Hot Plasma Composition Analyzer for the Magnetospheric Multiscale Mission. *Space Sci. Rev.* . doi: 10.1007/s11214-014-0119-6
- Zelenyi, L. M., Neishtadt, A. I., Artemyev, A. V., Vainchtein, D. L., & Malova, H. V. (2013, April). Quasiadiabatic dynamics of charged particles in a space plasma. *Physics Uspekhi*, *56*, 347-394. doi: 10.3367/UFNe.0183.201304b.0365
- Zhang, K., Li, X., Xiang, Z., Khoo, L. Y., Zhao, H., Looper, M. D., ... Sauvaud, J.-A. (2020). Long-term variations of quasi-trapped and trapped electrons in the inner radiation belt observed by demeter and sampex. *Journal of Geophysical Research: Space Physics*, *125*(9), e2020JA028086.
- Zhang, Q., Guo, F., Daughton, W., Li, H., & Li, X. (2021, October). Efficient Nonthermal Ion and Electron Acceleration Enabled by the Flux-Rope Kink Instability in 3D Nonrelativistic Magnetic Reconnection. *Phys. Rev. Lett.*, *127*(18), 185101. doi: 10.1103/PhysRevLett.127.185101
- Zhang, X.-J., Angelopoulos, V., Mourenas, D., Artemyev, A., Tsai, E., & Wilkins, C. (2022, May). Characteristics of Electron Microburst Precipitation Based

- on High-Resolution ELFIN Measurements. *Journal of Geophysical Research (Space Physics)*, 127(5), e30509. doi: 10.1029/2022JA030509
- Zhou, M., Ashour-Abdalla, M., Deng, X., El-Alaoui, M., Richard, R. L., & Walker, R. J. (2011, August). Modeling substorm ion injection observed by the THEMIS and LANL spacecraft in the near-Earth magnetotail. *Journal of Geophysical Research (Space Physics)*, 116(A8), A08222. doi: 10.1029/2010JA016391
- Zweibel, E. G., & Yamada, M. (2009, September). Magnetic Reconnection in Astrophysical and Laboratory Plasmas. *Annual Review of Astronomy and Astrophysics*, 47(1), 291-332. doi: 10.1146/annurev-astro-082708-101726